

Direct Contact vs. Solvent-shared Ion Pairs in NiCl₂ Electrolytes Monitored by Multiplet Effects at the Ni(II) L-edge X-Ray Absorption

Emad F. Aziz^{1}, Stefan Eisebitt¹, Wolfgang Eberhardt¹, Frank de Groot², Jau W. Chiou³, Chungi Dong³,
and Jinghua Guo³*

BESSY G.m.b.H.
Albert-Einstein Str. 15
12489 Berlin, Germany

Department of Inorganic Chemistry and Catalysis,
Utrecht University,
Sorbonnelaan 16, 3584,
The Netherlands.

Advanced Light Source Division,
Lawrence Berkeley National Laboratory,
94720 California,
USA.

*.Corresponding author: Emad.Aziz@bessy.de

Abstract

We investigate the local electronic structure in aqueous NiCl₂ electrolytes by Ni L edge x-ray absorption spectroscopy. The experimental findings are interpreted in conjunction with multiplet calculations of the electronic structure and the resulting spectral shape. In contrast to the situation in the solid, the electronic structure in the electrolyte reflects the absence of direct contact Ni-Cl ion pairs. We observe a systematic change of the intensity ratio of singlet and triplet-related spectral features as a function of electrolyte concentration. These changes can be described theoretically by a changed weight of transition matrix contributions with different symmetry. We interpret these findings as being due to progressive distortions of the local symmetry induced by solvent-shared ion pairs.

Introduction

Most properties of electrolyte solutions depend on the ability of solvent and solute to interact, and hence on the nature of the complex ion formation. One important property is the Gibbs free energy of solvation which requires an assumption on the effective ionic radii $r_{\text{ion}}^{\text{eff}}$ which is often expressed by $r_{\text{ion}} + \Delta R$. Here, ΔR is a function taking into account the first hydration shell¹. Due to the importance of ion behavior in electrolyte solutions, ions in electrolytes have been studied using many theoretical and experimental techniques. Molecular dynamics (MD) simulations, for instance, have shown that for 1M NaCl solution about 25% of the ions are included in neutral, solvent-shared clusters formed by a minimum of four ions.² MD studies have suggested an association of Na⁺ and Cl⁻ ions in solution via a two step mechanism, first establishing long distance ion-pairs separated by hydration shells, followed by direct contact ion-pair formation.^{3,4}

Several methods have been used to probe the local geometrical structure of ions in solution experimentally. In an X-ray diffraction study of saturated NiCl₂ solutions, Waizumi et al. have reported the existence of mixed-ligand chloroaqua octahedral complexes in addition to sixfold water coordinated Ni ions, i.e. the existence of direct contact ion pairs.⁵ A detailed picture for ion clustering in solution, including the solvent-shared hydration shell, has been given by Fulton et al.⁶ Based on their combined X-ray Absorption Near Edge Structure (XANES) and EXAFS studies, these authors have suggested a long-range interaction between Ca²⁺ and Cl⁻ in the solution which leads to a solvent-shared ion-pair (Ca²⁺-OH₂-Cl⁻). Direct contact ion-pairs between the cations and the anions have been argued to be negligible for CaCl₂ electrolyte solution even at high concentration. This is in agreement with a neutron diffraction study by Badyal et al.⁷, also providing evidence for the existence of solvent-shared ion-pairs.

For Ni²⁺ in aqueous solution, neutron diffraction studies^{8, 9} as well as X-ray diffraction⁵ have shown that Ni²⁺ has a coordination sphere of six water molecules. Inner sphere contact pairs of Ni-Cl have been suggested to exist for 8% of the Ni ions in a X-ray diffraction study of 3M NiCl₂ aqueous solution.¹⁰ X-ray diffraction of NiBr₂ aqueous solution has shown strong experimental evidence for ion-pair formation at 2M concentration within octahydration geometry.¹¹ Here we study the range from diluted (50 mM) to concentrated (1.5M) aqueous NiCl₂ solutions, where we expect a transition in the importance of interionic interactions.

Recently, we have studied the behavior of ions in the electrolyte solutions at ambient pressure and temperature, combining XANES with Density Functional Theory (DFT) simulations,¹² to investigate the effect of concentration,¹³ and solvent¹⁴ on the ion-ion interaction in aqueous NaCl solution. In this paper we present XANES spectra for the Ni²⁺ L-edge in aqueous NiCl₂ electrolyte solution as a function of the concentration, starting from the solid NiCl₂. Two distinctive spectral features can be assigned as fingerprints of direct contact ion-pairs and solvent-shared ion-pairs in the solution. The spectra have

been analyzed by the means of a charge transfer multiplet simulation.¹⁵⁻¹⁷ The multiplet approach has been extensively used in the analysis of L-edge spectra of transition metals, where it is established as a method for probing the metal ligand charge transfer.¹⁸⁻²¹

Experimental and Computational Techniques

The experiments were performed at two different light sources. First, measurements were conducted at the Advanced Light Source (ALS), Lawrence Berkeley National Laboratory, using the liquid end-station at beam line 7.0.1.²² In this end station, soft X-rays are coupled into a fixed volume liquid sample through a Si₃N₄ membrane of 100 nm thickness and lateral size of 1.0×1.0 mm. The sample holder was mounted in a vacuum chamber with a pressure of approximately $1 \cdot 10^{-9}$ mbar. The resolution of the beamline monochromator was set to be 0.3 eV at 850 eV. Further details about the experimental setup have been discussed before.^{23, 24}

The measurements were repeated using the LIQUIDROM flow jet end station at BESSY, Berlin, at beamline U41-PGM. The liquid was injected into the experimental chamber as a continuous flowing liquid jet. The interaction chamber is filled with 1 atm Helium, with the helium being continuously refreshed. The vacuum parts of the beam line were separated from the atmospheric helium setup via two stages of differential pumping, and a Si₃N₄ membrane of 100 nm thicknesses and lateral size of 0.5×0.5 mm. The resolution of the monochromator was set to be 0.2 eV at 850 eV.

In both experiments, the X-ray absorption spectra from liquid samples were recorded in fluorescence yield (FY) mode using a Gallium Arsenide photodiode of 5×5 mm² in size. The beamline energy was calibrated with respect to the 852 eV peak from a NiO single crystalline sample.

The samples were prepared from commercially available $\text{NiCl}_2 \cdot 6\text{H}_2\text{O}$ salts, purchased from Sigma-Aldrich. The powder has 99.8% purity, and was used without further purification. All Ni(II) solutions were freshly prepared before the experiment.

We use Charge Transfer Multiplet (CTM) calculations based on a combination of the Cowan code²⁵ for atomic multiplets, the crystal field program of Butler²⁶ and a charge transfer model Hamiltonian¹⁵ in order to calculate the electronic structure at the Ni site and the resulting XANES spectra. The calculations include the electronic Coulomb interactions and the spin orbit coupling on every open shell. The XANES spectra were simulated based on the crystal field strengths and the charge transfer parameters, as explained in detail before.¹⁵ All spectra shown in this work have been broadened by a Lorentzian of 0.2 eV and 0.3 eV for L_3 and L_2 edges, respectively, and a Gaussian of 0.25 eV in order to account for lifetime broadening and the experimental resolution, respectively.

There are several codes calculating the single particle X-ray absorption which can explain K-edge absorption well. Nevertheless, these codes typically agree poorly with the experiment in the case of the $L_{2,3}$ edge. The reason for this is that in general the density-of-states calculated theoretically is not observed in such an X-ray process. The density-of-states is affected by the strong overlap between the core wave function and the valence wave function. When the excitation takes place, the core orbitals are partially filled as in Ni(II) $2p^5$, and different pd multiplets can be excited. This multiplet effect was shown to be of the same order of magnitude in solids as it is in atoms.²⁷

For Ni(II), the multiplet interactions between the various possible core holes and the partly filled valence band have been demonstrated before.¹⁵ All s-core level excitations have been calculated ($1s^1 3d^9$, $2s^1 3d^9$, $3s^1 3d^9$) and it has been shown that the core hole multiplet contribution is negligible in these cases, and spin interaction between s-core hole and valence electron is the only significant coupling. For calculating the s-core level excitations, single electron codes are very effective. However, the multiplet interaction of the $2p^5 3d^9$ configuration for Ni(II) final state has a significant effect on the mixing of the

L₃ and L₂ edge, and the value of the Slater-Condon parameters is at least of the same order of magnitude as the spin-orbit coupling.

As we will see below, our experimental observations can be understood in a framework of distorted symmetry. Distortion of the local symmetry around the Ni ions influence which multiplet states can contribute to the spectra (depending on their symmetry). It is thus important to briefly discuss the symmetry of the involved states and operators on a group-theory basis.

In the X-ray absorption, the 2p core electron is transferred to 3d orbitals, and the transition can be described as $2p^63d^8 \rightarrow 2p^53d^9$. The ground state has 3F_4 symmetry and there are 12 term symbols for the final state (1P_1 , 1D_2 , 1F_3 , $^3P_{0,1,2}$, $^3D_{1,2,3}$, and $^3F_{2,3,4}$). The energy of the final states are described by the 2p3d Slater-Condon parameters, the 2p spin-orbit coupling and the 3d spin-orbit coupling. According to the selection rules, the 12 final states are reduced to 4 accessible final states 1F_3 , 3D_3 and $^3F_{3,4}$. By applying a cubic crystal field, the symmetry changes from spherical (SO₃) to octahedral (O_h), causing the p-orbital to be branched to a T_{1u} state. A d-orbital splits into E_g plus T_{2g} states. The dipole transition operator has p-symmetry on the atomic level, and by applying the crystal field, it branches to T_{1u} symmetry. The 3F wave function ground state is splitting into 3A_2 , 3T_1 and 3T_2 wave functions in O_h symmetry, where 3A_2 is the lowest energy state. In other words the eight 3d-electrons fill all T_{2g} states plus the two spin-up E_g states, leaving two spin-down E_g-holes. The symmetry of these two E_g-holes is written as 3A_2 . The CTM program works in double group symmetry, after the inclusion of spin-orbit coupling. This implies that the spin multiplicity must be branched as well. The 3A_2 state has S = 1, which is branched to T₁ in O_h symmetry. Applying spin-orbit coupling, i.e. multiplying T₁ and A₂ symmetry yields a T₂ overall symmetry ground state. Four dipole matrix elements as classified by their symmetry can contribute to the $2p^63d^8 \rightarrow 2p^53d^9$ transition, namely $\langle T_2|T_1|T_1\rangle$, $\langle T_2|T_1|E\rangle$, $\langle T_2|T_1|T_2\rangle$, and $\langle T_2|T_1|A_2\rangle$. The final spectra are then obtained as a linear superposition of these contributions. Charge transfer from Cl⁻ to Ni²⁺ is calculated by taking into account the $2p^63d^9L$ and $2p^53d^{10}L$

configurations (with L referring to a ligand hole), based on the Anderson impurity model²⁸⁻³³ and related short-range model Hamiltonians that are applied to core level spectroscopies.

Results and Discussion

In Fig.1, the Ni(II) L-edge electron yield XANES spectrum for NiCl₂ solid is presented as a reference for the liquid measurements. The 2p (L-edge) XANES spectrum of Ni(II) has a number of peaks that split into two main regions, one at 852 eV and one at 870 eV. The structures around 852 eV are related to the L₃ edge (P1 and P2 peaks). The features around 870 eV are related to the L₂ edge (P4 and P5 peaks); the 2p spin-orbit coupling leads to a splitting of approximately 18 eV. Peak P1 and peak P4 relate to a 2p⁵3d⁹ final state of triplet character, i.e. where the spins of the 2p shell and 3d electron are parallel. In contrast, peaks P2 and P5 relate to a singlet final state. A satellite peak above the L₃ edge at around 858 eV appears for the solid Ni(II) (P3 peak) The spectrum agrees well with published data by G. van der Laan et al.³² Within the L₃-edge, two peaks P1 and P2 split by 1.6 eV are observed. The satellite peak is known to be due to the Ligand Metal Charge Transfer (LMCT) from Cl⁻ to Ni²⁺,¹⁵ which is possible due to the close proximity of Ni and Cl in the solid. An overview spectrum for NiCl₂ aqueous solution is shown for comparison. As for all liquid spectra, XANES was measured by the fluorescence yield (FY). The changes in the peak intensities and splittings will be discussed as a function of concentration in the context of Fig.2

As a function of electrolyte concentration from 50 mM to 1500 mM, a systematic change in the XANES spectral features is observed as seen in Fig.2. Even at the highest concentration investigated, peak P3 is not detectable against the background noise level in the spectra of the electrolytes. The absence of this peak compared to the solid reflects the non-existing or at least strongly reduced amount of direct interaction between Ni²⁺ and Cl⁻ in the electrolyte solution as compared to the solid. However, given the slight uncertainty in the baseline, our results would still be consistent with 8% of Ni atoms in

direct-contact pairs with Cl^- , as reported for 3M NiCl_2 solution.¹⁰ As a second important difference between bulk and electrolyte spectra, the energy splitting within the L_3 edge in the electrolyte solutions is 2.4 eV compared to 1.6 eV for the solid. This increase of the L_3 splitting energy can be assigned to the absence of direct contact ion-pairs as well, as we will discuss later.

The most prominent intensity change is the increasing P2/P1 intensity ratio for increasing NiCl_2 concentration in the solvent. For geometrical reasons, FY-XANES spectra can exhibit distorted intensities if the edge absorption of interest is larger than the background absorption.^{34, 35} This effect becomes important in concentrated samples, and will be strong in solid NiCl_2 . For the solid, we have thus used XANES in electron yield (EY) mode to measure the absorption cross section (Fig.1), which due to its surface sensitivity does not suffer from these distortions. This approach is not feasible for the liquid samples. Here, we have quantified the concentration-dependent saturation effects. Based on the atomic absorption cross-sections we found the distortion to be negligible for 50 mM NiCl_2 solution. We calculate how the absorption cross section of the 50 mM solution would appear at elevated concentrations, which can be done analytically in conjunction with the known experimental geometry and atomic absorption cross sections.^{34, 35} These simulated spectra are presented in Fig.2 along with the measured spectra for different electrolyte concentrations.

Clearly, this geometrical saturation effect alone can not account for the observed intensity changes as a function of electrolyte concentration. It is the remaining effect of concentration on the XANES spectra which will be discussed in detail in this paper. It is evident from the XANES spectra that the electronic structure locally at the Ni(II) atoms in the solution changes as a function of electrolyte concentration. The change is such that peak P2 increases relative to P1 for increasing electrolyte concentration. Furthermore, a change in multiplet splitting energy was observed between solid and liquid spectra. In the following, we will rationalize these changes in the electronic structure on the basis of electronic structure calculations, where symmetry parameters are being varied.

In an XANES experiment, a spatial ensemble average over temporally frozen configurations is observed. Rigorously, such a system should be described by an ensemble average over a multitude of different local Ni environments in the liquid, obtained e.g. by molecular dynamics simulations. Here, we will follow a much simpler route and try to qualitatively understand the observed spectral changes analyzing one model. In order to simulate the observed spectral changes, multiplet calculations were performed, where Ni(II) in an O_h symmetric crystal field is considered. This approach is justified by the fact that the highly directed Ni d-orbitals favor a quite rigid local symmetry, as known from complex chemistry. For highly concentrated $NiCl_2$ solutions, local structural data was well described in O_h symmetry,⁵ as expected for Ni^{2+} with a d^8 electron configuration.

In Fig. 3 we display the simulated spectra obtained using a crystal field of 1.1 eV for the d^8 configuration, and a $d^9\bar{L}$ charge transfer state was included in order to describe the electron transfer from Cl^- to the valence d-orbitals of Ni(II). This configuration interaction with a contribution of the $d^9\bar{L}$ configuration of about 14% can explain the appearance of the P3 peak in the experimental spectra. This $d^9\bar{L}$ charge transfer can only be significant with Ni(II) and Cl^- being in direct contact, as in the solid $NiCl_2$. The significant reduction of the P3 peak intensity upon dissolving the solid $NiCl_2$ in water is consequently explained by the absence of $d^9\bar{L}$ charge transfer; that is, the Cl^- ions have moved out of Ni(II) in the first hydration shell. Furthermore, this treatment reproduces the experimentally observed P1-P2 peak energy splitting which is 1.6 eV for solid $NiCl_2$ and 2.4 eV for the solution. The simulated spectra have peak separations of 1.65 eV for mixed d^8 with $d^9\bar{L}$ configurations and 2.3 eV for a pure d^8 configuration. This implies that the ions in solution have rather weak charge transfer, since charge transfer compresses the multiplet splitting. The simulated spectra in Fig3 reproduce the experimental XANES spectra for the solid $NiCl_2$ well, including the spectral finger print (P3) for the existence of ion-pairs. Within pure O_h calculations, the change of the P2/P1 peak ratio in the salt solutions as a function

of concentration (Fig. 2) can not be reproduced. Only the most dilute 50 mM Ni(II) solution can be described in perfect O_h symmetry with a pure d^8 configuration.

In order to explain the change of the fluorescence yield as a function of Ni(II) concentration, we would like to mention that the calculated absorption for d^8 configuration in an O_h crystal field consist of four dipole matrix element components added equally e.g. $\langle f|p|i\rangle = \alpha \langle T_2|T_1|T_1\rangle + \beta \langle T_2|T_1|E\rangle + \sigma \langle T_2|T_1|T_2\rangle + \phi \langle T_2|T_1|A_2\rangle$, where α , β , σ and ϕ are = 1. The origin of these transition dipole matrices has been discussed in detail in the computational method part of this paper. We observe that in order to reproduce the experimental XANES spectra for Ni^{2+} solution as a function of concentration, these four matrix elements are added not equally. Furthermore, Analysis shows that the main channels for the singlet states (855 eV, 872 eV) have T_1 character, while the triplet $2p^5 3d^9$ states (853 eV, 870 eV) have mixed T_2 , E and A_2 character. This implies that one can simulate the variation in triplet (P1 peak) versus singlet (P2 peak) states by varying the ratio of the different coefficients α through ϕ , and in particular by varying α with respect to the remaining coefficients.

In Fig. 4, we plot the resulting variation of the spectral shape of the coefficients α through ϕ , within limits such that the overall spectral shape starts to become unphysical for the extreme values of α and σ . This defines a variation interval from 0.5 to 3.0, outside this interval the overall intensity ratio of L_3 -related vs. L_2 -related peaks is clearly disagreeing with the experimental spectra in the literature and in this work. Over this parameter interval, both the $\langle T_2|T_1|T_1\rangle$ and $\langle T_2|T_1|T_2\rangle$ matrix elements show a strong variation of the P2/P1 intensity ratio, with an inverted sign of the intensity ratio dependence on α and σ , respectively. A variation of α from 3.0 to 0.5 while keeping the other coefficients constant at 1.0 does reproduce the variation in spectral shape that is observed experimentally, i.e. it increases the P2/P1 peak intensity ratio. Consequently, linear combinations with variation of all four coefficients can generate theoretical spectra which describe the experimental findings as a function of electrolyte

concentration well. The change of the relative contributions of the $\langle T_2 | T_1 | T_1 \rangle$ matrix elements to the total transition probability reflects a changing weight of the spectral contribution of the triplet state versus the singlet state. The fact that we can explain the experimentally observed changes in the Ni L XANES spectra by this procedure suggests that the change of the singlet/triplet ratio may be the most significant change of the electronic structure at the Ni site induced by the increase of the ion concentration in the electrolyte.

This interpretation is based on experimental electronic structure XANES data in comparison to the multiplet calculations of the spectral shape in O_h symmetry and with distortions which one would encounter e.g. if the crystal field strength on one high symmetry axis would be changed relative to the two remaining high symmetry axes. The theory does not rely on particular structural models of the ions and solvent molecules in the electrolyte beyond symmetry arguments. From an atomistic point of view, one would expect reduced interionic correlation lengths for increasing electrolyte concentration. When approaching a saturated aqueous $NiCl_2$ solution (4.6 M at RT), one might expect to see evidence of direct contact $Ni^{2+} Cl^-$ ion pairs, as reported by Waizumi et al.⁵ Even at 1.5 M concentration, we find no appreciable weight of direct contact ion pairs as evidenced by the lack of intensity at the P3 peak position. This leads us to conclude that the changes in the local electronic structure at the Ni^{2+} site as a function of electrolyte concentration must be due to indirect, solvent-shared, ion-pair (or ion cluster) formation. In a simple picture one could describe our findings as evidence of local distortions due to indirect ion-pairs, with increasing distortion for increasing ion concentration in the electrolyte. These distortions manifest themselves in the ensemble average of quasi-frozen configurations during the X-ray absorption interaction time via the multiplet field experienced by the Ni(II) ion. The concept of solvent-shared ion-pairs is in line with EXAFS and neutron diffraction studies, where a long range arrangement of oppositely charged ions in solution via shared solvation shells was observed.^{6, 7}

Summery

A consistent picture for the changes of the local electronic structure at Ni(II) in NiCl₂.aq electrolyte has been developed by combining experimental L-edge Ni(II) XANES spectra with multiplet calculations of the electronic structure. While spectra for solid NiCl₂ show an unambiguous fingerprint of charge transfer made possible by direct Ni-Cl contact, such a feature is absent in the spectra of the electrolytes. In addition, the energy splitting between the first two absorption beaks within the L₃ edge (P1 and P2) is increased from from 1.6 eV in the solid to 2.4 eV in the electrolyte. With increasing electrolyte concentration, the P2/P1 intensity ratio increases. These changes in peak energies and intensities are reproduced by a multiplet calculation of the Ni XANES spectra in O_h symmetry by a variation of the relative contributions of the dipole matrix elements with different symmetry (T₁ vs. A₂, T₂ and E). This is equivalent to an increased contribution of singlet states versus the triplet states for increasing electrolyte concentration. We relate these changes in the electronic structure to the increasing importance of solvent-shared ion pairs at elevated electrolyte concentrations, manifesting itself in a progressive distortion of the local O_h symmetry around the Ni ions.

ACKNOWLEDGMENTS

We are grateful to the user support teams at ALS and BESSY for their valuable aid. The ALS work was supported by the Director, Office of Science, Office of Basic Energy Sciences, and Biosciences of the U.S. Department of Energy at Lawrence Berkeley National Laboratory under contract No. DE-AC02-05CH11231.

Figure Captions

FIG. 1: Nickel L-edge EY-XANES spectrum for solid NiCl₂ (black), and FY-XANES for NiCl₂ 1500 mM (red).

FIG. 2: Nickel L₃-edge FY-XANES spectra for NiCl₂ solution as a function of the concentration. For comparison, the 500 mM sample spectrum (blue) was measured in the static cell (line with circles), and in the liquid flow jet (solid line). A simulation of the saturation effect due to the fluorescence detection mode is presented under each spectrum (red solid line), the difference to the experimental data at the P2 peak has been shaded. If the electronic structure would **not** change with concentration, the FY-XANES spectra would appear like the simulated spectra. This effect is geometrical in nature and solely due to the influence of saturation.

FIG. 3: Calculated Ni(II) L-edge XANES spectra using 1.1 eV crystal field. (a) For pure d⁸ configuration, (b) For 86% d⁸ configuration mixed 14% d⁹L configuration. Calculated states are indicated by sticks and have been broadened by 0.25 eV and 0.3 eV lorentzian for L₂ and L₃ edges respectively, and 0.25 eV Gaussian.

FIG. 4: Hypothetical Ni(II) L₃-edge XANES spectral shape upon variation of the different transition matrix contributions. Spectra are calculated for a crystal field of 1.1 eV and pure d⁸ configuration. The relative weight of (a) α, (b) β, (c) σ, (d) φ has been varied from 0.5 (black) to 3 (blue). The resulting spectra have been normalized on the P1 peak.

References

- (1) Marcus, Y., Linear Solvation Energy Relationships - a Scale Describing the Softness of Solvents. *Journal of Physical Chemistry* **1987**, 91, (16), 4422-4428.
- (2) Degreve, L.; da Silva, F. L. B., Large ionic clusters in concentrated aqueous NaCl solution. *Journal of Chemical Physics* **1999**, 111, (11), 5150-5156.
- (3) Koneshan, S.; Rasaiah, J. C., Computer simulation studies of aqueous sodium chloride solutions at 298 K and 683 K. *Journal of Chemical Physics* **2000**, 113, (18), 8125-8137.
- (4) Dang, L. X.; Chang, T. M., Molecular mechanism of ion binding to the liquid/vapor interface of water. *Journal of Physical Chemistry B* **2002**, 106, (2), 235-238.
- (5) Waizumi, K.; Kouda, T.; Tanio, A.; Fukushima, N.; Ohtaki, H., Structural studies on saturated aqueous solutions of manganese(II), cobalt(II), and nickel(II) chlorides by X-ray diffraction. *Journal of Solution Chemistry* **1999**, 28, (2), 83-100.
- (6) Fulton, J. L.; Heald, S. M.; Badyal, Y. S.; Simonson, J. M., Understanding the effects of concentration on the solvation structure of Ca²⁺ in aqueous solution. I: The perspective on local structure from EXAFS and XANES. *Journal of Physical Chemistry A* **2003**, 107, (23), 4688-4696.
- (7) Badyal, Y. S.; Barnes, A. C.; Cuello, G. J.; Simonson, J. M., Understanding the effects of concentration on the solvation structure of Ca²⁺ in aqueous solutions. II: Insights into longer range order from neutron diffraction isotope substitution. *Journal of Physical Chemistry A* **2004**, 108, (52), 11819-11827.
- (8) Soper, A. K.; Neilson, G. W.; Enderby, J. E.; Howe, R. A., Neutron-Diffraction Study of Hydration Effects in Aqueous-Solutions. *Journal of Physics C-Solid State Physics* **1977**, 10, (11), 1793-1801.
- (9) Neilson, G. W.; Enderby, J. E., Hydration of Ni²⁺ in Aqueous-Solutions. *Journal of Physics C-Solid State Physics* **1978**, 11, (15), L625-L628.

- (10) Magini, M., Hydration and Complex-Formation Study on Concentrated-Solutions Co(II)Cl₂ Ni(II)Cl₂ Cu(II)Cl₂ by X-Ray-Diffraction Technique. *Journal of Chemical Physics* **1981**, 74, (4), 2523-2529.
- (11) Caminiti, R.; Cucca, P., X-Ray-Diffraction Study on a NiBr₂ Aqueous-Solution - Experimental-Evidence of the Ni(II)Br Contacts. *Chemical Physics Letters* **1982**, 89, (2), 110-114.
- (12) Hermann, K.; Pettersson, L. G. M.; Casida, M. E.; Daul, C.; Goursot, A.; Koester, A.; Proynov, E.; St-Amant, A.; R., S. D.; Carravetta, V.; Duarte, H.; Godbout, N.; Guan, J.; Jamorski, C.; Leboeuf, M.; Malkin, V.; Nyberg, M.; Pedocchi, L.; Sim, F.; Triguero, L.; Vela, A. *StoBe-deMon version 1.0*, 2002.
- (13) Aziz, E. F.; Zimina, A.; Freiwald, M.; Eisebitt, S.; Eberhardt, W., Molecular and electronic structure in NaCl electrolytes of varying concentration: Identification of spectral fingerprints. *Journal of Chemical Physics* **2006**, 124, (11), -.
- (14) Aziz, E. F.; Freiwald, M.; Eisebitt, S.; Eberhardt, W., Steric hindrance of ion-ion interaction in electrolytes. *Physical Review B* **2006**, 73, (7), -.
- (15) de Groot, F., Multiplet effects in X-ray spectroscopy. *Coordination Chemistry Reviews* **2005**, 249, (1-2), 31-63.
- (16) Rehr, J. J.; Ankudinov, A. L., New developments in the theory of X-ray absorption and core photoemission. *Journal of Electron Spectroscopy and Related Phenomena* **2001**, 114, 1115-1121.
- (17) Rehr, J. J.; Albers, R. C., Theoretical approaches to x-ray absorption fine structure. *Reviews of Modern Physics* **2000**, 72, (3), 621-654.
- (18) Hu, Z.; Kaindl, G.; Warda, S. A.; Reinen, D.; de Groot, F. M. F.; Muller, B. G., On the electronic structure of Cu(III) and Ni(III) in La₂Li_{1/2}Cu_{1/2}O₄, Nd₂Li_{1/2}Ni_{1/2}O₄, and Cs₂KCuF₆. *Chemical Physics* **1998**, 232, (1-2), 63-74.
- (19) Hu, Z.; Mazumdar, C.; Kaindl, G.; de Groot, F. M. F.; Warda, S. A.; Reinen, D., Valence electron distribution in La₂Li_{1/2}Cu_{1/2}O₄, Nd₂Li_{1/2}Ni_{1/2}O₄, and La₂Li_{1/2}Co_{1/2}O₄. *Chemical Physics Letters* **1998**, 297, (3-4), 321-328.

- (20) Okada, K.; Kotani, A., Complementary Roles of Co 2p X-Ray Absorption and Photoemission Spectra in Co. *Journal of the Physical Society of Japan* **1992**, 61, (2), 449-453.
- (21) Hocking, R. K.; Wasinger, E. C.; de Groot, F. M. F.; Hodgson, K. O.; Hedman, B.; Solomon, E. I., Fe L-edge XAS studies of K-4[Fe(CN)(6)] and K-3[Fe(CN)(6)]: A direct probe of back-bonding. *Journal of the American Chemical Society* **2006**, 128, (32), 10442-10451.
- (22) Warwick, T.; Heimann, P.; Mossessian, D.; Mckinney, W.; Padmore, H., Performance of a High-Resolution, High-Flux Density Sgm Undulator Beamline at the Als (Invited). *Review of Scientific Instruments* **1995**, 66, (2), 2037-2040.
- (23) Guo, J. H.; Luo, Y.; Augustsson, A.; Kashtanov, S.; Rubensson, J. E.; Shuh, D.; Zhuang, V.; Ross, P.; Agren, H.; Nordgren, J., The molecular structure of alcohol-water mixtures determined by soft-X-ray absorption and emission spectroscopy. *Journal of Electron Spectroscopy and Related Phenomena* **2004**, 137-40, 425-428.
- (24) Guo, J. H.; Augustsson, A.; Kashtanov, S.; Spangberg, D.; Nordgren, J.; Hermansson, K.; Luo, Y.; Augustsson, A., The interaction of cations and liquid water studied by resonant soft x-ray absorption and emission spectroscopy. *Journal of Electron Spectroscopy and Related Phenomena* **2005**, 144-147, 287-290.
- (25) Cowan, R. D., *The Theorey of Atomic Structure and Spectra*. ed.; University of California Press: Berkeley, California, 1981; 'Vol.' p.
- (26) Butler, P. H., *Point Group Symmetry, Applications, Methods and Tables*. ed.; New York: New York, 1991; 'Vol.' p.
- (27) Degroot, F. M. F., X-Ray-Absorption and Dichroism of Transition-Metals and Their Compounds. *Journal of Electron Spectroscopy and Related Phenomena* **1994**, 67, (4), 529-622.
- (28) Jo, T.; Kotani, A., Narrowing Due to Valence Mixing in the 3d Core Level Spectra for Ce Compounds. *Journal of the Physical Society of Japan* **1988**, 57, (7), 2288-2291.
- (29) Gunnarsson, O.; Schonhammer, K., Electron Spectroscopies for Ce Compounds in the Impurity Model. *Physical Review B* **1983**, 28, (8), 4315-4341.

- (30) Fujimori, A.; Minami, F., Valence-Band Photoemission and Optical-Absorption in Nickel Compounds. *Physical Review B* **1984**, 30, (2), 957-971.
- (31) Sawatzky, G. A.; Allen, J. W., Magnitude and Origin of the Band-Gap in Nio. *Physical Review Letters* **1984**, 53, (24), 2339-2342.
- (32) Vanderlaan, G.; Zaanen, J.; Sawatzky, G. A.; Karnatak, R.; Esteva, J. M., Comparison of X-Ray Absorption with X-Ray Photoemission of Nickel Dihalides and Nio. *Physical Review B* **1986**, 33, (6), 4253-4263.
- (33) Zaanen, J.; Sawatzky, G. A.; Allen, J. W., Band-Gaps and Electronic-Structure of Transition-Metal Compounds. *Physical Review Letters* **1985**, 55, (4), 418-421.
- (34) Eisebitt, S.; Boske, T.; Rubensson, J. E.; Eberhardt, W., Determination of Absorption-Coefficients for Concentrated Samples by Fluorescence Detection. *Physical Review B* **1993**, 47, (21), 14103-14109.
- (35) Degroot, F. M. F.; Arrio, M. A.; Saintavit, P.; Cartier, C.; Chen, C. T., Fluorescence Yield Detection - Why It Does Not Measure the X-Ray-Absorption Cross-Section. *Solid State Communications* **1994**, 92, (12), 991-995.

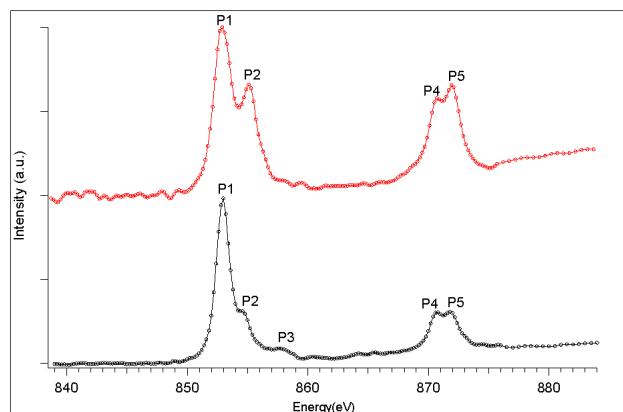


Figure 1.

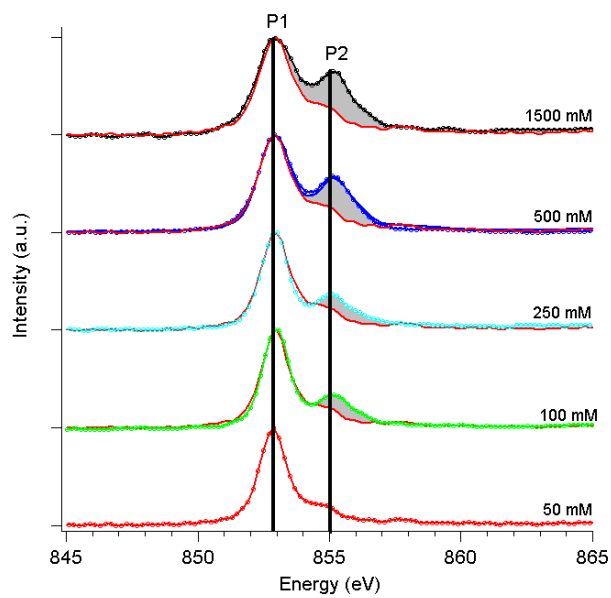


Figure 2.

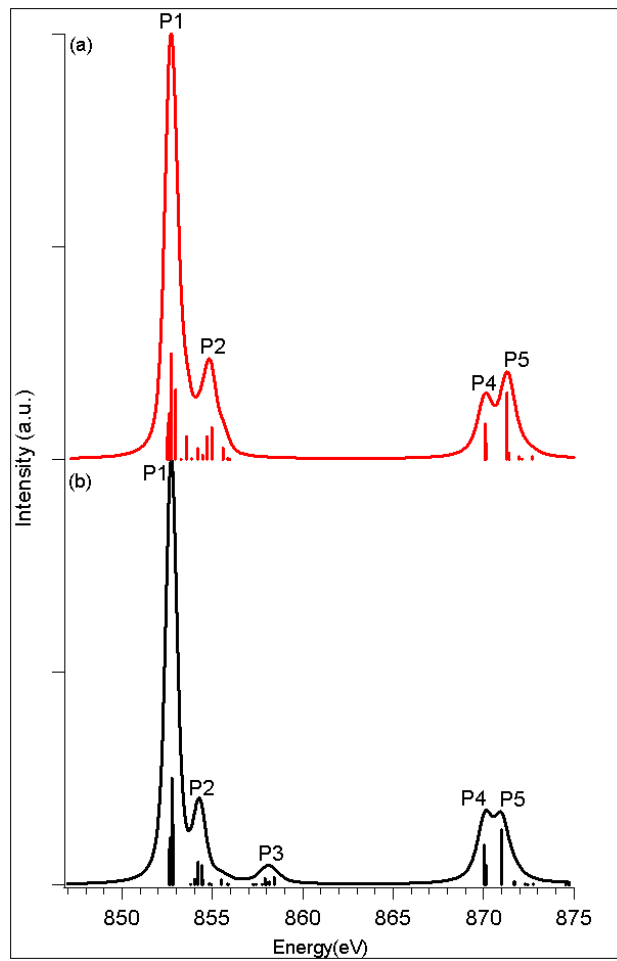


Figure 3.

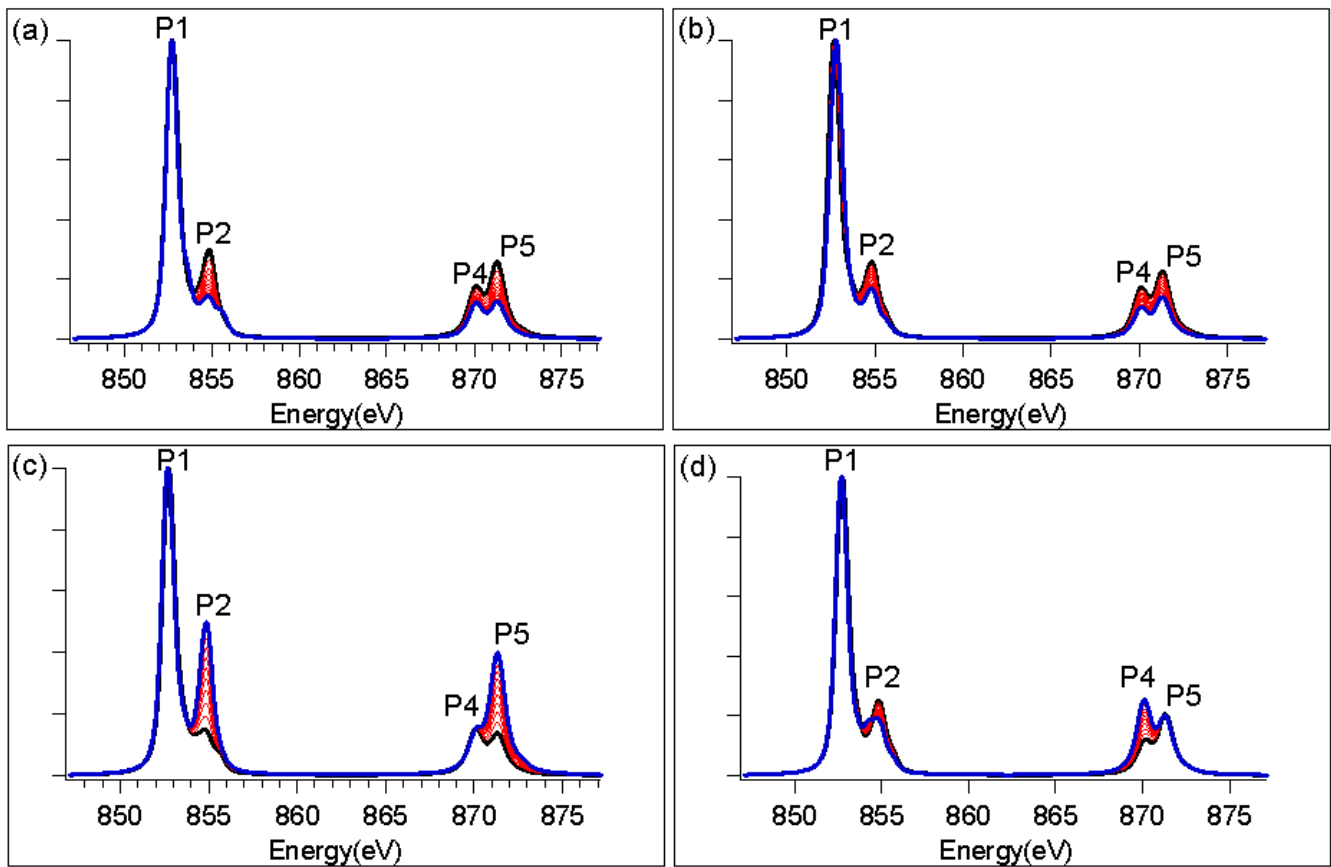
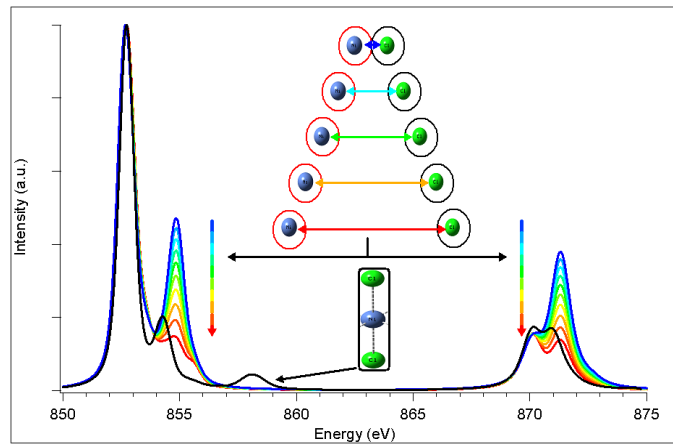


Figure 4.



TOC